Field emission from carbon nanotubes: perspectives for applications and clues to the emission mechanism

J.-M. Bonard*, **J.-P. Salvetat, T. Stöckli, L. Forró, A. Châtelain**

Département de Physique, Ecole Polytechnique Fédérale de Lausanne, CH-1015 Lausanne, Switzerland
(E-mail: jean-marc.bonard@epfl.ch)

Abstract. We report on the extensive characterization of carbon nanotube electron field emitters. We studied the emission behavior of single-wall, closed and opened arc-discharge multi-wall, and catalytically grown multi-wall nanotubes, as single emitters and in film form. The nanotube field emitters show excellent field emission properties, but significant differences were observed between the different types of nanotubes. To obtain good performances as well as long emitter lifetimes, the nanotubes should be multi-walled and have closed, well-ordered tips. Complementary results such as energy distribution and luminescence induced by the field emission give further precious indications on the field emission mechanism. The large field amplification factor, arising from the small radius of curvature of the nanotube tips, is partly responsible for the good emission characteristics. Additional evidence however shows that the density of states at the tip is non-metallic, appearing in the form of localized states with well-defined energy levels.

PACS: 61.48.+c; 79.70.+q; 73.20 Dx

Although most of the research conducted on multi-wall and single-wall carbon nanotubes since their discovery in 1991 [1] and 1993 [2] has been of a fundamental nature, a keen interest is shown for their potential applications. Numerous "Gedanken" devices incorporating nanotubes have thus been proposed, and the variety and originality of the different ideas are an eloquent testimony of the imagination of the scientists working in the field. Apart from applications that may be realized in a distant future only, carbon nanotubes have shown great potential in some domains. For example, they have proven to be extremely stiff and resistant to bending [3], and their suitability as a tip for scanning probe microscopy has been demonstrated [4]. They also rank among the best electron field emitters that are now available [5–17].

Electron sources are widely used nowadays, both in research and in industry, and rely mostly on thermoelectronic emission, meaning that the electrons are emitted from a heated filament. In research, more and more instruments demand sources with high brightness and monochromatic emission, and call for the use of field emission sources. We will show in this report that a single carbon nanotube can readily be used in high-resolution electron beam instruments.

In the industry, there is a great market potential for field emission sources in cathode ray tubes (for giant displays, for example) as well as in flat panel displays. It is extremely encouraging to see that such devices incorporating nanotubes have already been demonstrated, by Saito et al. [15] for cathode ray tubes and by Wang et al. [12] for a 32×32 pixel display. With the progress made in the catalytic growth of nanotubes, which permits a patterned growth on a substrate [16], and with the excellent field emission properties of nanotube films that will be outlined below, there is little doubt that commercial devices based on carbon nanotubes electron sources will one day hit the market.

In this paper, we will assess the potential of carbon nanotubes as field emitters by studying some of the most important parameters for field emission sources: the voltages required for emission (Sect. 2), the current stability (Sect. 3), and the energy spread (in Sect. 4, along with a discussion of the emission mechanism), both for single nanotube emitters and for film emitters. In this respect, we also compare the properties of the different types of nanotubes. It is well known that carbon nanotubes appear in a fascinating variety of forms, with one or several graphitic sheets, with closed or opened tips, with well-ordered (graphitic) or disordered structure. The influence of these structural properties on the field emission has not been evaluated yet, but may prove important for applications. The four types of nanotubes studied here are shown in the transmission electron microscopy (TEM) images of nanotube tips of Fig. 1. First, single-wall nanotubes (SWNTs) have a mean diameter of ≈ 1.4 nm, lengths that can reach several microns, and end in a spherical cap: they are thus among the sharpest inorganic objects found in nature. SWNTs are mostly found assembled in ropes with a triangular lattice. Second, closed multi-wall nanotubes (MWNTs) as produced by the arc discharge, which have typically 5 to 10 times larger diameters, and show tips with a polyhedral shape. Third, opened MWNTs, with their tips removed by

* Corresponding author
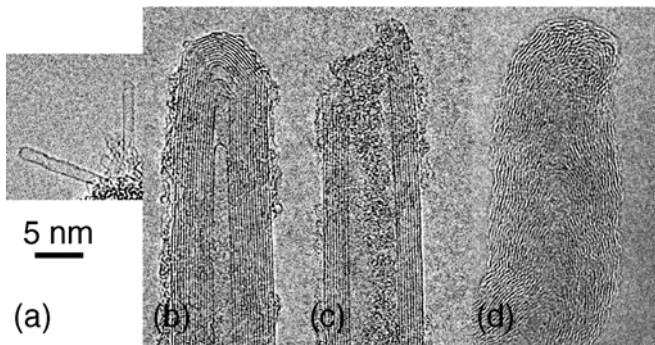
Fig. 1a–d. Transmission electron microscopy images of carbon nanotube tips for a **a** SWNT (mean diameter: ≈ 1.4 nm), **b** closed arc-discharge MWNT (14 ± 5 nm), **c** opened arc-discharge MWNT (15 ± 6 nm), **d** catalytically grown MWNT (22 ± 7 nm). All images are reproduced at the same final magnification

oxidation, and consequently exposed graphitic layers and inner cavity. Finally, MWNTs produced by catalytic reactions, which show in our case large diameters and partially ordered layers containing extended structural defects, with graphitic planes tilted with an angle of about 30° with respect to the tube axis and forming a piled-up "coffee-cup" structure.

1 Emitter fabrication

1.1 Production of carbon nanotubes

MWNTs were produced in a carbon arc apparatus using the method described by Ebbesen and Ajayan [18], i.e., by arc discharge between two graphite electrodes ($U = 16$ V, $I = 80$ A) in a 350-mbar He atmosphere. When needed, these MWNTs were opened by heating in air at 550 °C for 1 h and 620 °C for 12 min [19].

The arc-discharge yields, along with carbon nanotubes, nanoparticles consisting of nested closed graphitic layers of polyhedral shape. It is important for field emission to have good quality samples with as little "foreign" material as possible. For MWNTs, we have developed a soft purification method which uses the properties of colloidal suspensions [20]. We start the purification with a suspension prepared from 500 ml distilled water, 2.5 g sodium dodecyl sulfate (a common surfactant), and 50 mg of MWNT arc powder sonicated during 15 min. Sedimentation and centrifugation (at 5000 rpm for 10 min) removes all graphitic flakes larger than 500 nm from the solution, as confirmed by low-magnification SEM observations. We then add 10 g surfactant to the solution. At such surfactant concentrations, micelles form and induce flocculation, i.e., the formation of aggregates. These aggregates contain mainly large objects, while smaller objects remain dispersed, and sediment after a certain time, typically a few hours. After decanting the suspension for about one week, we repeat the procedure once or twice. While the as-deposited material contains a large proportion of nanoparticles (typically 70% in number and 40% in weight), the sediment contains nanotubes with a content of over 90% in weight. Most closed arc-discharge MWNT emitters were realized with purified nanotubes, yielding lower emission voltages as compared to as-deposited arc-discharge material, probably because the large graphitic flakes screen

the applied field and reduce the field amplification on the emitting tubes.

The SWNTs were produced by arc discharge under 500-mbar He static pressure using pure graphite electrodes. A 3-mm hole was drilled in the anode and filled with a graphite-Ni-Y mixture with weight proportion 2 : 1 : 1 [21]. The voltage and current used were approximately 25 V and 100 A. The nanotubes were predominantly found in the webs, as opposed to the cathodic deposit.

The disordered nanotubes were produced by catalytic decomposition of acetylene on reduced cobalt oxide deposited on a silica substrate [22]. The nanotube powder was collected after dissolution of the silica substrate and catalyst in acid. In this case, the nanotubes showed a high density of structural defects.

1.2 Single nanotube field emitter

To realize a field emission source with one nanotube only, we mounted single MWNTs on a supporting gold wire (diameter 20 μm) that was electrolytically etched to a ≈ 250-nm-radius tip with a procedure similar to the one described in [4]. No adhesive was used, and the tubes were held onto the tip by Van der Waals forces. The tips were systematically characterized by SEM, as in Fig. 2a. Note that the tip needs not to have one single tube, since the emission from the second-best-placed tubes will not contribute significantly to the emitted current.

1.3 Nanotube film field emitter

The nanotube films were realized by drawing a colloidal suspension of nanotubes through a 0.2-μm pore silica filter, and by transferring this film on a teflon-coated metal surface [5]. The emission surfaces ranged from 0.1 to 25 mm^2 and are easily upscalable. This simple and fast preparation method can furthermore be used for all types of nanotubes, in contrast to catalytic deposition techniques [14, 16], and has the advantage of being non-destructive, which is not the case for alternative film preparation techniques where the tubes are opened [7]. Figure 3 shows typical SEM micrographs of pristine films. The morphology of the films varied much with
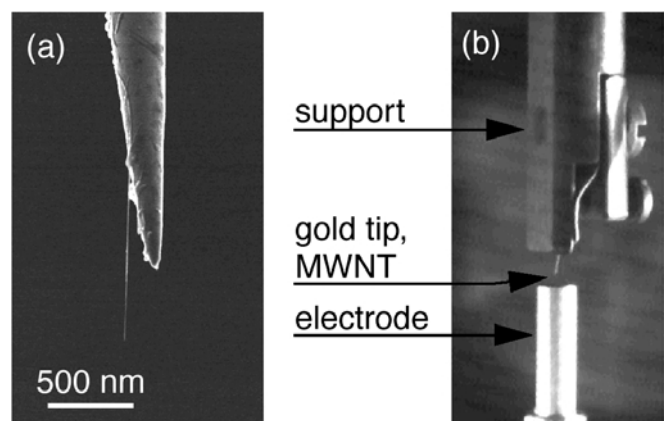
Fig. 2. a Single MWNT mounted on the tip of an etched gold wire. **b** Optical micrograph of the experimental setup for field emission: the gold wire is fixed on a support, and placed 1 mm above the cylindrical counter-electrode
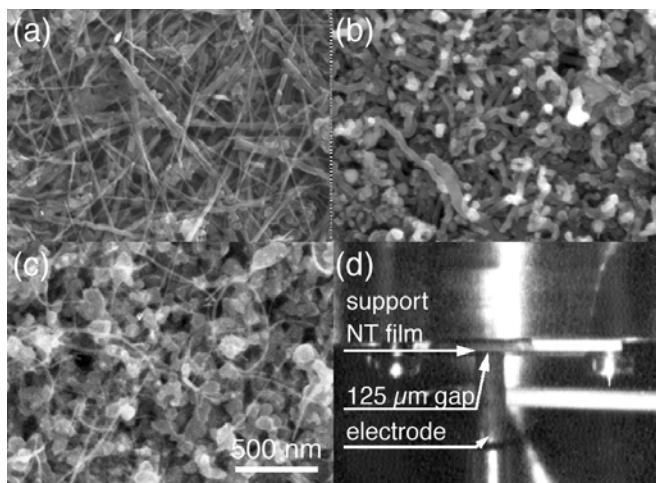
Fig. 3. **a**–**c** SEM images of nanotube films taken at the same magnification: **a** closed arc-discharge MWNTs, **b** catalytically grown MWNTs, **c** SWNTs. Films incorporating opened MWNTs are comparable to image (**a**). **d** Optical micrograph of the experimental setup for field emission: the metal platelet which supports the film is mounted face-down on a support, and placed at 125 μm distance from the cylindrical counter-electrode

the type of the nanotubes. The arc-discharge MWNT films (Fig. 3a) were composed of thin, straight and long tubes, while the catalytic tubes (Fig. 3b) were far thicker and curved. As for the SWNT films (Fig. 3c), they were composed of single tubes and ropes lying on the surface along with catalyst particles coated with amorphous carbon. The average nanotube density amounted to typically $10^9 \, \text{cm}^{-2}$.

1.4 Experimental setup

For field emission, a 3-mm-diameter cylindrical counter-electrode was placed at a distance of 1 mm for the single tube emitters and 125 μm for the film emitters (Fig. 2b and Fig. 3d, respectively). A Keithley 237 source-measure unit was used for sourcing the voltage (up to 1000 V) and measuring the current (with pA sensitivity), allowing the characterization of the current–voltage ($I - V$) behavior. The measurements were carried out at pressures of 10^{-7} mbar unless said otherwise.

2 Emitter characteristics

2.1 Single nanotube field emitter

Figure 4a displays a typical $I - V$ characteristic for a single MWNT (in this case an opened MWNT). At low currents, the $I - V$ characteristics followed a Fowler–Nordheim (F–N) behavior (i.e., elastic tunneling through a triangular barrier, with the electron distribution described by Fermi–Dirac statistics [23], which describes quite accurately electron field emission from metallic emitters). This can be seen in the inset of Fig. 4a where $\ln(I^2/V)$ is plotted as a function of $1/V$ (a so-called F–N plot): a F–N behavior is characterized by a constant slope in such a plot. Depending on the sample, the "metallic behavior" persisted up to 5–20 nA of emitted current.
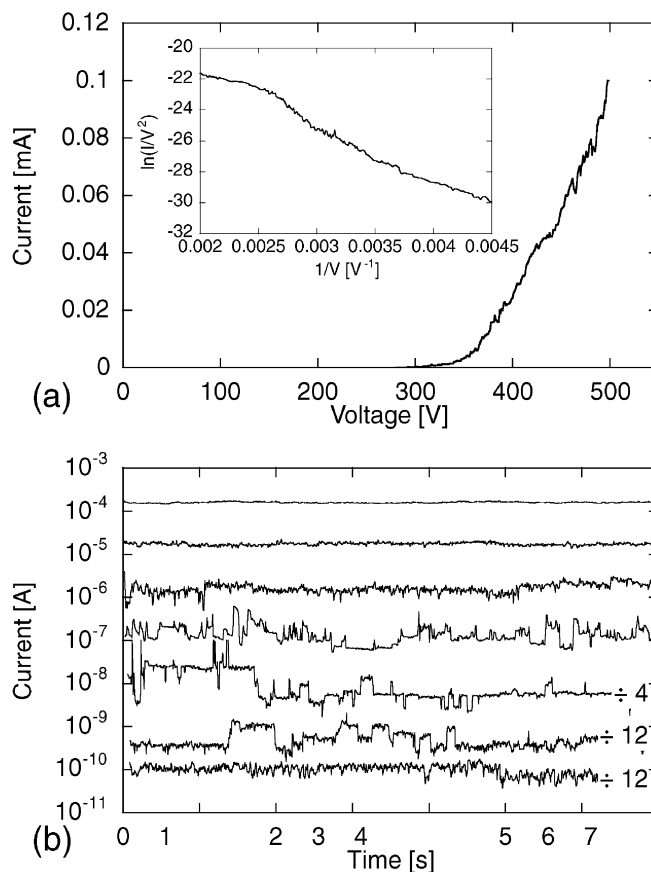
Fig. 4. **a** $I - V$ characteristics for a single opened MWNT, with in inset the corresponding Fowler–Nordheim plot. **b** Current stability versus time for the tube of Fig. 4a. The time scale for the three lowest traces has been divided by a factor 12, 12 and 4, respectively

At higher currents, the slope changed (by typically 10%–30%), increasing or decreasing depending on the sample, without discontinuities or instabilities in the $I - V$ characteristics up to ≈ 0.1 μA. A very strong saturation with large instabilities followed by an abrupt step was sometimes observed [10] when the voltage was further increased. Most emitters, such as the MWNT of Fig. 4, showed a strong decrease of the F–N slope corresponding to a saturation around 1 μA emitted current.

It is worth noting that most single MWNT emitters, closed as well as opened, are capable of emitting over an incredibly large current range. The maximum current we succeeded to draw from one nanotube was ≈ 0.2 mA, and MWNTs reached routinely and repeatedly 0.1 mA. This represents a tremendous current density for such a small object, and is actually quite close to the theoretical limit where the tube should be destructed by resistive heating [10]. This experimental limit is comparable to the one observed by other groups that studied the electronic transport properties of MWNTs [24, 25].

In Fig. 4b, we report current stability measurements for the tube of Fig. 4a over the whole explored current range (≈ 10 pA to 0.1 mA). We observed two different current regimes. At low currents, switching between discrete levels occurred. The frequency of switching between the steps increased with the current, with periods of stable emission covering more than 60 s at low currents (see Fig. 4b, bottom-most trace).
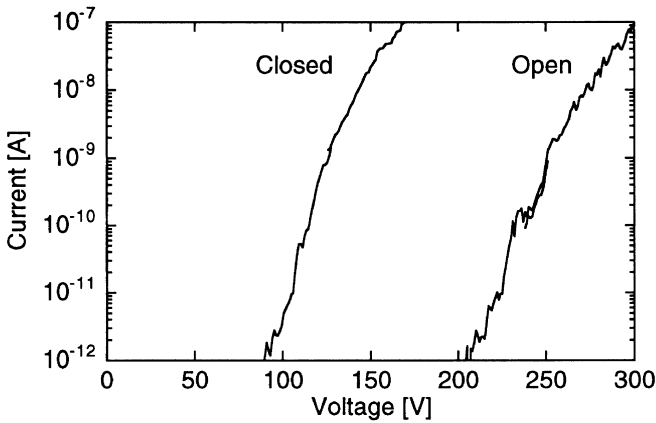
Fig. 5. $I - V$ characteristics for a single closed and opened MWNT (the current is given in logarithmic scale)

This switching regime persisted up to 0.1–1 µA, depending on the tube. At higher currents, stable emission with flicker noise was observed, with the signal-to-noise (S/N) ratio increasing with the current. The stability increased further when the emitters were operated in ultrahigh vacuum (10^{-9} mbar).

No significant difference was observed between closed and opened MWNT save for the most important property: the voltage needed for the emission. In Fig. 5, we compare the $I - V$ performances of a closed and opened MWNT. We noted for all measured samples that opened tubes were far less efficient emitters than as-grown tubes. The voltages needed for a given emission current are typically a factor 2 higher for the opened tubes. In effect, open edges like those depicted in Fig. 1b may have smaller radius of curvature than closed ends, and opened tubes would be expected to emit current at lower applied voltages due to the higher field amplification. Quite surprisingly, the emission characteristics of nanotubes are seriously degraded by opening their ends.

2.2 Nanotube film field emitter

The behavior of the films is readily comparable to the single emitters, as can be seen in Fig. 6 for a SWNT film. At low currents, Fowler–Nordheim behavior was observed up to emitted current densities of 0.1–10 µA cm^{-2} (Fig. 6a), with the F–N slope changing slightly at higher currents. At 10–100 µA cm^{-2}, a distinct diminution of the F–N slope (and therefore saturation) occurred on all samples.

The current stability at constant applied voltage (Fig. 6b) depended again on the current (not on the applied voltage), and presented different current regimes. At low currents (< 10–25 µA cm^{-2}), current switching between discrete current levels was observed. The switching frequency increased with the current, with periods of stable emission as long as 240 s. At currents higher than 10 µA cm^{-2} (which corresponded approximately to the saturation point), the emission became gradually stable, without any detectable discrete levels with our time resolution of 10 ms. The signal-over-noise ratio increased with the current.

We compare in the following the field emission performances of the four different types of nanotubes. Useful parameters for such a comparison are the turn-on field, E_{to} and the threshold field E_{thr}, i.e., the electric field (voltage
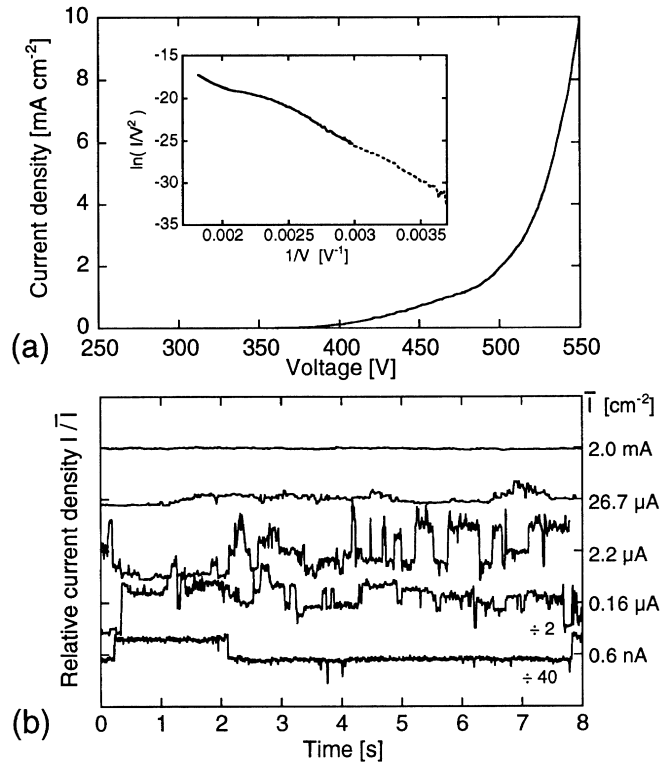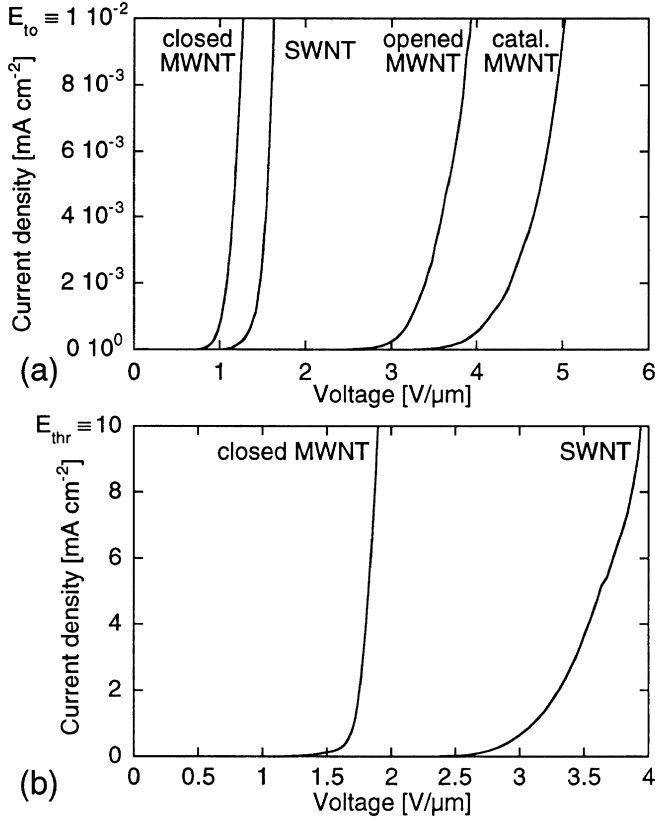

Fig. 6. a $I - V$ characteristics for a SWNT film with in inset the corresponding Fowler–Nordheim plot. *Solid* and *dotted lines* correspond to different ranges of the source-measure unit. **b** Current stability versus time for the tube of Fig. 6a. The time scale for the two lowest traces has been divided by a factor 40 and 12, respectively

over interelectrode distance V/d) to produce a current density of 10 µA cm^{-2} and 10 mA cm^{-2}, respectively. These figures of merit correspond to typical values encountered in panel display applications. In Fig. 7, we display $I - V$ characteristics around E_{to} (a) and E_{thr} (b). We found systematically that closed MWNT films displayed lower emission voltages, followed by SWNTs, opened MWNTs and finally catalytic MWNTs.

We list in Table 1 the average values for E_{to} and E_{thr} obtained on at least five films for each type of nanotube (top part), as well as the values obtained on MWNT films by other groups along with our best devices (bottom part). Several conclusions can be drawn from this comparison. First, there are roughly two categories of tubes with respect to the needed emission voltages: closed MWNTs and SWNTs, with $E_{to} < 2.7$ V/µm and $E_{thr} < 5$ V/µm, and opened and catalytic MWNTs, with $E_{to} > 5$ V/µm and $E_{thr} > 15$ V/µm. In particular, we note again that opened MWNTs are far less efficient emitters than closed MWNTs. Finally, our values compare readily to those obtained by other groups for opened MWNT films [9] and catalytically grown nanotube arrays [16]. However, both emitter fabrication methods yielded tubes aligned with their axis perpendicular to the substrate, which results in a higher field amplification at the nanotube tips and thus in lower operating voltages.

To discuss further the observed differences between the different types of nanotubes, we estimate the field amplification factor β from the $I - V$ characteristics and corresponding F–N plots. This field amplification factor depends only on the geometrical shape of the emitter for a given work function

Fig. 7a,b. $I-V$ characteristics around **a** the turn-on field E_{to} and **b** the threshold field E_{thr} for different nanotube films

proportion. In the following, we estimate the field amplification factor from the F–N slope in the low-current regions, by taking $\phi = 5\,eV$: we are aware that this is valid only as an approximation, but it allows us nevertheless to compare the different emitters.

We report in Table 2 the field amplification factor estimated from the constant F–N slope in the low-current regime averaged over five samples or more. The field amplification factors were significantly higher for single- than for multiwall nanotubes films. This enhancement is most probably due to the smaller tip radius of SWNTs. The tip radius is also responsible for the low field amplification obtained with the catalytic tubes with respect to the closed MWNTs, although the disordered structure of the tip and the high defect density may also have an influence. However, the difference between closed and opened MWNTs cannot only arise from geometrical considerations, since the variation of mean diameter and length between opened and closed MWNT is rather small (see Fig. 1). We speculate that most of this difference is due to changes in the work function that arise from the state of the tip (see also next section). In fact, the 1.5-fold decrease of β would correspond to a 1.3-fold increase in ϕ. Energy distribution measurements will be undertaken in the future to clarify this issue.

In summary, our catalytic tubes showed high emission voltages mainly because of their larger average diameter. The small diameter of SWNT should lead to very low emission voltages, whereas the SWNT films show "only" comparable performances to closed MWNT films. We suppose that this relative inefficiency arises from the fact that most SWNTs are bundled in ropes, and that these ropes mostly end in catalyst particles. Only few SWNT tips are detected by TEM, and these protrude only by a few tens of nm at most from the sample, as in Fig. 1a. This in turn means that the density of free SWNT tips, and thus of potential emission centers, is far lower than for MWNTs. As for the huge difference between closed and opened MWNTs, we noted that our best film emitter with opened tubes didn't even come close in performances to the worst emitter with closed tubes. The observed difference can therefore not be assigned to the quality of the films, and we conclude that it is due in great part to the state of the tip.

2.3 Comparison with other film emitters

In comparison with other field emitters, the applied voltages needed for field emission with nanotubes were far lower for a comparable emitted current, as can be inferred from Table 3 where the turn-on field and the threshold field of diamond and amorphous carbon films and of our best emitter are reported. Other film emitters show comparable turn-on fields, but far

ϕ and interelectrode distance d. In the frame of the Fowler–Nordheim model [23], the slope of the F–N plot is equal to $B\phi^{3/2}d/\beta$, where $B = 6.87 \times 10^9\,V\,eV^{-3/2}\,m^{-1}$. The field amplification factor is defined as $F = \beta V/d$, where F is the field just above the surface of the tip, and V the applied voltage.

One difficulty here is that the workfunction is not known a priori. It is possible to determine both ϕ and β by performing energy distribution measurements; it is in fact the only reliable way to evaluate the workfunction. This has been performed only very recently for MWNTs. A value of 7.3 eV was found for one arc-discharge MWNT [17], and the work function for a catalytic MWNT film has been reported to be 5.3 eV [14]. Further work is however needed to establish if the work function varies from one tube to the next and in what

Table 1. Turn-on (E_{to}) and threshold (E_{thr}) fields in V/μm for various nanotube film field emitters. Top part: average values from this work. Bottom part: values obtained by other groups and our best devices

Emitter	E_{to}	E_{thr}	
Arc MWNT	2.6	4.6	
Arc SWNT	2.7	5.2	
Opened MWNT	4.5	30	
Catalytic MWNT	5.6	14	
Opened MWNT	0.9	3.7	[9]
Catalytic MWNT	n.a.	4.8	[16]
Closed MWNT	1.1	2.2	This work, best device
SWNT	1.5	3.9	This work, best device

Table 2. Average field amplification factor β on nanotube films

Emitter	Field amplification factor
SWNT films	3400
closed MWNT films	1600
opened MWNT films	1100
catalytic MWNT films	830

Table 3. Turn-on (E_{to}) and threshold (E_{thr}) fields in V/µm for various film field emitters. The asterisk, *, denotes values extrapolated from $I - V$ characteristics

Emitter	E_{to}	E_{thr}	Reference
Diamond	24*	40*	[26]
Diamond B doped	16*	30*	[26]
Diamond N doped	1.5	≫ 8*	[27]
Diamond tips (gold-coated)	3	22*	[28]
CVD diamond on Si tips	1.5*	3.4	[29]
Amorphous carbon (ta-C)	3	≫ 25*	[30]
MW nanotubes	1.1	2.2	this work

higher threshold fields. Furthermore, most of the cited values, especially for E_{thr}, are extrapolated from low-current measurements, which implies that the effective values may be far higher. Nanotubes compare well to other film emitters primarily because of their high aspect ratio, which results in a large field amplification factor.

We note that the only emitters that compete in terms of emission voltage with nanotubes films are the diamond-covered Si tips realized by Zhirnov et al. [29]. This indicates that maximum efficiency for film field emitters can be reached only when the emitters are well aligned and placed with their long axis perpendicular to the film substrate, and when the emitters are well separated from one another. These conditions are naturally realized in Spindt tips arrays (Mo tips deposited on a Si substrate [31]), which are, up to now, the only industrially viable film field emitters. We thus infer that carbon nanotube films will have to be realized fulfilling the above-mentioned conditions to reach a maximum emitting efficiency. To our knowledge, the only method to grow aligned and well-separated nanotubes is by catalytic reactions over a patterned substrate, as currently investigated by several groups [14, 16, 32]. Our results suggest however that care should be taken to obtain well-graphitized, closed MWNTs with small diameters.

3 Emitter degradation

3.1 Single nanotube field emitters

We noted in the previous section that carbon nanotubes show excellent field emission performances, with what are to our knowledge the lowest values for turn-on and threshold fields. However, although the operation voltage is an important parameter for applications, the key factor is long-term stability. The degradation of the emitting performances can be readily evaluated by measuring the evolution of emission intensity at constant applied voltage. For single closed MWNT tips, stable emission was observed for more than 90 h at 2 µA emission current ($U = 300$ V). Typical behavior of metallic cold field emitters, i.e., a gradual and reversible decrease due to the formation of absorbed layers, was not observed. Termination of the emission happened on most tips as a catastrophic and irreversible failure. This event was unpredictable, but occurred usually after a period of increasing instabilities. For opened MWNTs, the emission also stopped abruptly, but after shorter time spans than for their closed counterparts. Furthermore, their emission was often unstable, with abrupt decreases/increases.

The maximum current that we succeeded to draw from one MWNT was ≈ 0.2 mA. At such elevated currents, the emission current was stable for a few seconds before a catastrophic failure of the emission. This irreversible degradation occurred in less than 10 ms (time resolution of the measurement), without any preceding current increase, and resulted probably from resistive heating of the MWNT [10].

It is worth noting that lifetimes of more than 1400 h have been reported for emission in ultrahigh vacuum (better than 4×10^{-9} mbar) for one single tube emitting at 0.5 µA [17].

3.2 Nanotube film field emitters

A gradual degradation of the emission performances with time was detected on all film emitter samples [10, 13]. $I - V$ characteristics acquired at different degradation stages showed furthermore a monotonous decrease of the field amplification factor, and observations by SEM on films after emission revealed a substantial decrease of the tube density.

A comparison between different nanotube films at comparable chamber pressure and emitted current density, as on Fig. 8a and Table 4, shows clearly that the degradation was significantly faster (a factor 10) for SWNTs. It is most probable that the tubes were gradually destroyed, mainly through ion bombardment (by gas phase electron ionization or by ion desorption from the anode, both induced by the emitted electrons). It is not surprising that SWNTs show faster degradation than MWNTs. The single shell of SWNTs makes them
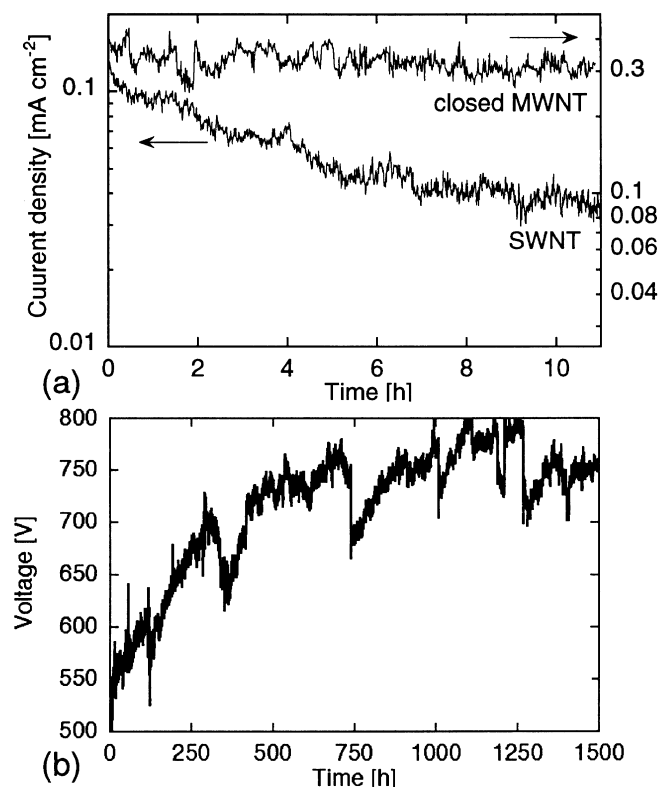
Fig. 8. a Long-term emission stability at constant applied voltage for a closed MWNT and a SWNT film. The extent of the y axis is the same for both films. **b** Long-term emission stability at a constant emitted current of 3 mA cm^{-2} for a closed MWNT film

Table 4. Average halftimes, in hours, at $0.2\,\mathrm{mA\,cm^{-2}}$ emitted current density for different nanotube films

Emitter	Halftime /h
SWNT	12.8
catalytic MWNT	10
opened MWNT	20
closed MWNT	120

more sensitive to bombardment or irradiation, whereas the multiple shells of MWNTs tend to stabilize their structure in this respect.

Table 4 compares the average degradation halftimes τ (obtained by fitting an exponential, $\exp(-t/\tau)$, to the current versus time curve) for different nanotube films at the same chamber pressure and emitted current density. It appears that closed MWNT are by far the most robust emitters: they degrade more than 10 and 6 times slower than catalytic and opened MWNTs, respectively. This difference can only be ascribed to the crystalline structure of the tip, which suggests that the tube ends have to be closed and well-ordered in order to maximize the emitter lifetime. Indeed, the structure of closed nanotube tips is characterized by a far lower density of dangling bonds, which minimizes the possibility of surface self-diffusion and adsorption.

Factors other than the type of the tubes influence the degradation [10], such as the chamber pressure and the emitted current density. As for the single tube emitters, longer lifetimes were observed in ultrahigh vacuum. However, we also saw that carbon nanotube emitters are still able to operate in a vacuum of 2×10^{-2} mbar [10].

Finally, the degradation seems to lessen after a certain operation time. We report in Fig. 8b a life-test over more than 1500 h (about two months), where the emission current was kept constant at $3\,\mathrm{mA\,cm^{-2}}$ and the applied voltage was allowed to vary. The voltage increased steadily for the first half of the test, then levelled out and remained on average at a nearly constant value.

4 Energy spread and emission mechanism

4.1 Energy spread

One of the advantages of field emission electron sources is that the energy spread is far lower than for thermoelectronic sources. In macroscopic metal emitters, where the emitted electrons come from the conduction band below the Fermi level, the width of the distribution (full width at half maximum, or FWHM) is essentially defined by the tunnelling barrier. The energy spread can be as low as 0.3 eV, but typical values are in the 0.45 eV range [17, 33].

Figure 9a shows a typical energy distribution obtained on a closed MWNT film just at the onset of emission. The FWHM is in this case 0.18 eV only, and we observed an average FWHM over 10 samples of 0.2 eV, without taking into account the broadening due to the finite resolution of the energy analyzer. The energy spread of MWNTs is thus at least half that of metallic emitters. Such low energy spreads are more comparable to ultrasharp emitters where the emis-
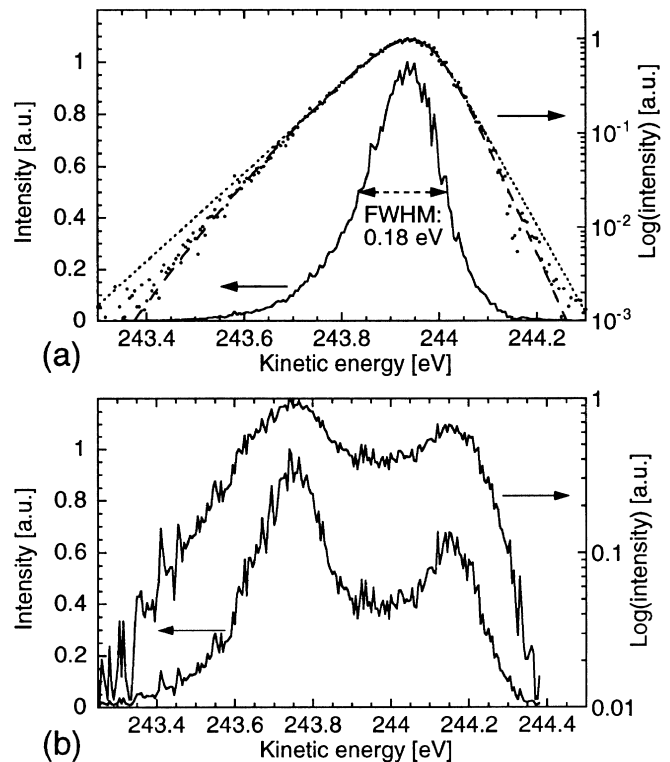
Fig. 9a,b. Field electron energy spectra obtained on a MWNT film (with a linear and logarithmic current scale for the bottom and top trace, respectively), showing **a** a single peak, along fits obtained with the F–N distribution (*dotted line*) and with the modified F–N distribution including a Gaussian band of states (*dashed line*); **b** two peaks

sion occurs from well-defined emitting states as opposed to a metallic continuum [33].

According to the Fowler–Nordheim theory, the energy distribution of the emitted electrons is $I_{FN}(E) \propto \exp((E - E_f)/b(F/\phi^{1/2})) \times f(E - E_f)$, where E is the electron energy, E_f the Fermi energy, and $f(E)$ the Fermi–Dirac distribution. We show in the top trace of Fig. 9a the best fit obtained on this spectrum with the F–N distribution (dotted line). Obviously, the distribution does not match the measured spectrum. The F–N theory predicts exponential slopes on both sides of the distribution arising from the tail of the Fermi–Dirac distribution and from the increase of the barrier width, respectively, which are not observed here.

To obtain good agreements with the measured spectra, we consider a Gaussian band of states at the tip of the tubes instead of the usual metallic density of states (DOS), resulting in a distribution $I_E = I_{FN}(E) \times \exp(-(E - E_c)^2/(\Delta E)^2)$, i.e., the Fowler–Nordheim distribution times a Gaussian band of width ΔE centered at an energy E_c. With this distribution, the tube body, which supplies the tip states (Gaussian band) with electrons, is taken as metallic, i.e., with a DOS described by the Fermi–Dirac statistics. This modified formula fits well the spectra, as can be seen in Fig. 9a (dashed line), and allows one to estimate the width of the Gaussian (typically 0.2–0.4 eV) and the Fermi temperature of the electrons (300–400 K).

The shape of the energy distribution of MWNTs therefore strongly suggests that the electrons are not emitted from a metallic continuum, but from energy bands of 0.2–0.4 eV width. We also found the presence of several narrow peaks on some spectra as displayed in Fig. 9b. The FWHM of the

peaks was also on the order of 0.2 eV, and they were separated by typically 0.5 eV. Such a situation may arise either when one tube has two energy bands separated by a fraction of an eV, or when two tubes are emitting at the same time. In the latter case, the difference in energy between the peaks would not come from a potential difference, but because the bands are not located at the same energy from one tube to the next. Interestingly, such multiple-peaked spectra have been observed by another group on one single tube, with comparable FWHM and peak separation [17].

4.2 Field-emission-induced luminescence

A rather unusual behavior linked to the field emission was observed in the form of light emission on single- and multi-wall nanotubes films as well as on single MWNT emitters. The light emission occurred in the visible part of the spectrum, and could sometimes be seen with the naked eye. This luminescence was induced by the electron field emission since it was not detected without applied potential (and thus emitted current).

The emitted light intensity followed furthermore closely the variations in emitted current. Actually, the emitted intensity depends critically on the current, since the relative variations are $3-4$ times higher for the luminescence as compared to the current. To investigate further this phenomenon, we analyzed the spectral distribution of the emitted light for single MWNTs. A typical spectrum is displayed in Fig. 10a. The spectra could be described with very good accuracy as a sum of two Gaussian functions, with peak energies, widths, and relative intensities that varied with experimental conditions. The FWHMs in the case of Fig. 10a were 0.34 eV and 22 meV for the broad and the narrow Gaussian, respectively, with an integrated intensity ratio of typically 20. No significant changes in the shape of the spectra were observed when the current was varied apart from a small shift (< 25 meV) of the broad Gaussian. As for the luminescence intensity I_p as a function of the emitted current I, it followed a power law $I_p \propto I^{\alpha}$ with $\alpha = 1.4 \pm 0.2$ in the case of the tube of Fig. 10a, as can be seen on Fig. 10b. The position and width of the narrow Gaussian remained nearly constant from one tube to the next. As for the broad Gaussian contribution, we observed peak intensities and widths varying between 1.73 and 1.83 eV and between 0.3 and 1 eV, respectively. Finally, light was emitted at higher energies from SWNTs as compared with MWNTs.

There has been one report of observed luminescence on opened nanotubes [6] but it was attributed to an incandescence of carbon chains at the tip of the tube provoked by resistive heating. Our results however strongly suggest that the light emission is directly coupled to the field emission. The narrowness of the luminescence lines and the very small shifts with varying emitted current show that we are not in presence of blackbody radiation or of current-induced heating effects, but that photons are emitted following transitions between well-defined energy levels.

Actually, the dependence of I_p versus I can be reproduced by a simple two-level model [34], where the density of states at the nanotube tip is simplified to a two-level system, with the main emitting level at energy E_1 below or just above the Fermi energy, and a deep level at $E_2 < E_1$. When an electron is emitted from the deep level, it is replaced either by an electron from the tube body, or by an electron from the main level which can provoke the emission of a photon. From the Fowler–Nordheim model, the transition probability $D(E)$ can be evaluated for each level, and in the frame of our model, $I \propto D(E_1)$, $I_p \propto D(E_2)$. It appears that I_p varies as a power of I with an exponent that depends on the separation of the levels [34], and that amounts to $1.51 - 1.65$ for the energies observed here (typically 1.8 eV), which corresponds well to the experimental observations.

These observations again strongly suggest the presence of energy levels, and thus of localized states, at the tip. We estimate that one emitted photon corresponds to at least 10^6 field-emitted electrons. With localized states at the tip, the greatest part of the emitted current will arise from occupied states with a large local density of states located near the Fermi level. Other, more deeply located electronic levels may also contribute to the field emission. In this case, the emitted electron will be replaced either by an electron from the semi-metallic tube body with an energy comparable to the level energy, or by a tip electron from the main emitting state. Clearly, the second alternative may provoke the emission of a photon. Although the tunneling probability for electrons from deeper state is several orders of magnitude lower than for the main emitting state, it will be readily sufficient to cause the observed light intensities.
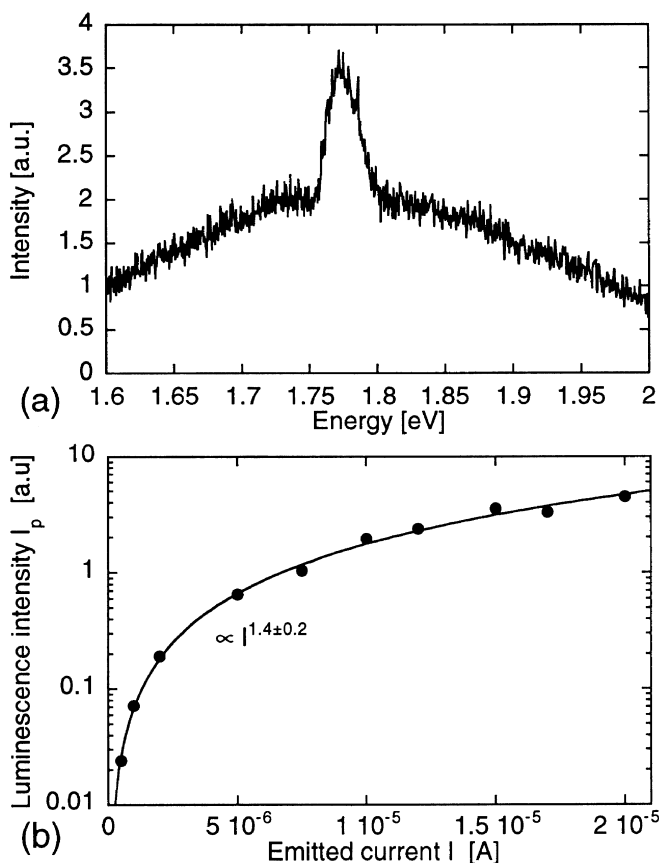
Fig. 10. a Spectrum of field emission induced luminescence for one MWNT emitter at 20 μA emitted current; **b** Luminescence intensity as a function of the emitted current (*dots*) along with a power law fit (*solid line*)

4.3 Field emission microscopy

Field emission microscopy (FEM) is an extension of field emission characterization, which offers a unique possibility of visualizing the spatial distribution of the emitted current by replacing the counter-electrode with a phosphor screen. We performed FEM on SWNT films (with the emission area reduced to 0.1 mm diameter). A simple $20\times$ magnifying electrostatic lens, held at about 1 mm distance, was used as counter-electrode, and a phosphor screen located 5 cm above the film-lens assembly allowed us to visualize the field emission patterns. The FEM patterns observed on the screen reflect directly the emitted current distribution. Since the tunneling electrons have very small kinetic energy, they follow the lines of forces, which diverge in first approximation radially from the emitter surface. The emission pattern at the tip, reflecting the spatial distribution of the emitted density, is thus enlarged before hitting the screen. A pattern detected by FEM on carbon nanotubes can be induced either by adsorbates, by local changes in the emitted current due to preferential emission sites (surface steps that result in a locally enhanced field amplification, protrusions of amorphous carbon present on the tip surface, or atomic wires), or spatial variations of the electronic density.

Figure 11 shows a sequence of field emission patterns recorded at ≈ 1 s intervals. On the films, several spots were usually simultaneously visible on the screen. Beside single spots and elongated and/or circular features without any distinctive shape, some well-defined patterns were observed. Most of them acted definitely as a unit. Like the one outlined in the first frame of Fig. 11, they abruptly changed shape, rotated, or disappeared suddenly. This behavior makes it highly plausible that each of these patterns is due to a single tip, or to a single adatom/admolecule. Individual patterns of two-fold and four-fold symmetry were frequently observed evolving from simple spot patterns, but no three- or five-fold symmetry patterns were detected [35]. More complicated figures consisting of a series of fringes (up to four) showing two-fold symmetry, with some fringes divided in two leafs, were also observed. Because of the observed symmetries, it is very improbable that the different spots on the patterns were caused by preferential emission from protrusions of amorphous carbon, single atomic wires, or surface steps. On metallic tips, absorbates also give rise to two- or four-fold leaf patterns, appearing bright and superimposed on the usual tip pattern. However, complicated patterns like the ones on Fig. 11 were only very rarely detected, whereas they systematically appear at high current for nanotubes, and no additional tip pattern was observed in superposition. Furthermore, experiments carried out in ultrahigh vacuum conditions after applying a high positive voltage (field evaporation) [35] or after heating in ultra high vacuum [17] yielded comparable results [35]. It is thus most probable that the observed patterns are caused solely by spatial variations of the electronic density, i.e., that
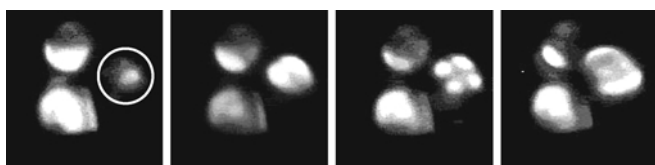

Fig. 11. Sequence of field emission patterns obtained on a SWNT film

they reflect the electronic density of the emitting states at the tip. The fact that the electronic distribution from a single tube shows a non-homogenous structure points again to the fact that the electrons are emitted from electronic states localized at the tip, and are not delocalized conduction-band electrons as in metals.

4.4 Field emission mechanism

The results presented in Sect. 2 show that the large field amplification factor, arising from the small radius of curvature of the nanotube tips, is partly responsible for the good emission characteristics. It is however still unclear whether the sharpness of nanotubes is their only advantage over other emitters, or if intrinsic properties also influence the emission performances.

Most authors conclude that carbon nanotubes are metallic emitters [9, 11], essentially because the $I - V$ characteristics seem to follow the Fowler–Nordheim law. The results presented above show however systematic deviations from the Fowler–Nordheim model at high emitted currents. Such deviations are usually attributed to space-charge effects [36] which induce a diminution of the F–N slope at fields F higher than 7 V/nm. For nanotubes, changes in the F–N slope occurred mostly at 4 V/nm, and typically at 2.5 V/nm already. This suggests that in our case space-charge effects were not the dominant cause for the deviations from the F–N model, and that nanotubes cannot be considered as usual metallic emitters.

Further observations such as those presented in Sect. 4 confirm this conclusion, and strongly suggest that the electrons are not emitted from a metallic continuum as in usual metallic emitters, but rather from well-defined energy levels of ≈ 0.3 eV half-width corresponding to localized states at the tip. First, the energy spread of nanotubes is typically half that of metallic emitters (about 0.2 eV), and the shape of the energy distribution suggests that the electrons are emitted from narrow energy levels. Second, the observation of luminescence coupled to the field emission indicates that several of these levels participate in the field emission: although the greatest part of the emitted current comes from occupied states with a large density of states near the Fermi level, other, deeper levels also contribute to the field emission.

In fact, theoretical calculations and STM measurements on SWNTs and MWNTs show that there is a distinctive difference in the electronic properties between the tip and the cylindrical part of the tube. For MWNTs, the tube body is essentially graphitic [37], whereas SWNTs display a characteristic DOS [38, 39] that reflects their one-dimensional character [40]. In contrast, the local density of states at the tip presents sharp localized states that are correlated to the presence of pentagons [35, 37, 39]. Interestingly, the FWHM of these states and their separation is readily compatible with our observations.

We conclude that the greatest part of the emitted current comes from occupied states close below the Fermi level. The position of these levels with respect to the Fermi level, which depends primly on the tip geometry [37] (i.e., tube chirality and diameter and the eventual presence of defects), would be, together with the tip radius, the major factor that determines the field emission properties of the tube. Indeed, only tubes

with a band state close under or just over the Fermi level are good candidates for field emission.

Finally, it is worth noting that the presence of such localized states influences greatly the emission behavior. At and above room temperature, the body of MWNTs behave essentially as graphitic cylinders. This means that the carrier density at the Fermi level is very low, i.e., on the order of 5×10^{18} cm^{-3}, which is 3 orders of magnitude less than for a metal. Simulations show that the local density of states at the tip reaches values at least 30 times higher than in the cylindrical part of the tube. The field emission current would be far lower without these localized states for a geometrically identical tip since it depends directly on this carrier density. The crystalline structure influences also strongly the position and intensity of the localized states, which could explain the superiority of closed over opened or disordered MWNTs. Another complementary explanation for this observation is that the coupling of the tip states to the metallic body is probably far better for closed MWNTs, leading to an increased electron supply and thus higher emitted current.

5 Conclusions

We performed systematic studies of field emission on carbon nanotubes of different types and confirm their excellent field emission performances. We observed significant differences in the emission characteristics between single-wall, closed and opened arc-discharge multi-wall, and catalytically grown multiwall nanotubes. To obtain low operating voltages as well as long emitter lifetimes, the nanotubes should be multi-walled and have closed, well-ordered tips. SWNTs degrade substantially faster, as do MWNTs with disordered structures. Finally, the emission performances of MWNT nanotubes are seriously degraded by opening their ends.

Our results give further precious indications on the field emission mechanism. The large field amplification factor, arising from the small radius of curvature of the nanotube tips, is partly responsible for the good emission characteristics. Additional evidence however shows that the density of states at the tip is non-metallic, appearing in the form of localized states with well-defined energy levels, and that the presence of such states influences greatly the emission behavior.

References

1. S. Iijima: Nature **354**, 56 (1991)
2. S. Iijima, T. Ichihashi: Nature **363**, 603 (1993); D.S. Bethune, C.H. Kiang, M.S. Devries, G. Gorman, R. Savoy, J. Vazquez, A. Beyers: Nature **363**, 605 (1993)
3. M.R. Falvo et al.: Nature **389**, 582 (1997); J.-P. Salvetat, G.A.D. Briggs, J.-M. Bonard, R.R. Bacsa, A.J. Kulik, T. Stöckli, N.A. Burnham, L. Forró: Phys. Rev. Lett. **82**, 944 (1999)
4. H. Dai, J.H. Hafner, A.G. Rinzler, D.T. Colbert, R.E. Smalley: Nature **384**, 147 (1996)
5. W.A. de Heer, A. Châtelain, D. Ugarte: Science **270**, 1179 (1995)
6. A.G. Rinzler, J.H. Hafner, P. Nikolaev, L. Lou, S.G. Kim, D. Tomanek, P. Nordlander, D.T. Colbert, R.E. Smalley: Science **269**, 1550 (1995)
7. P.G. Collins, A. Zettl: Appl. Phys. Lett. **69**, 1969 (1996)
8. H. Schmid, H.-W. Fink: Appl. Phys. Lett. **70**, 2679 (1997)
9. Q.H. Wang, T.D. Corrigan, J.Y. Dai, R.P.H. Chang, A.R. Krauss: Appl. Phys. Lett. **70**, 3308 (1997)
10. J.-M. Bonard, F. Maier, T. Stöckli, A. Chatelain, W.A. de Heer, J.-P. Salvetat, L. Forró: Ultramicroscopy **73**, 7 (1998)
11. Y. Saito, K. Hamaguchi, K. Hata, K. Tohji, A. Kasuya, Y. Nishina, K. Uchida, Y. Tasaka, F. Ikazaki, M. Yumura: Ultramicroscopy **73**, 1 (1998)
12. Q.H. Wang, A.A. Setlur, J.M. Lauerhaas, J.Y. Dai, E.W. Seelig, R.P.H. Chang: Appl. Phys. Lett. **72**, 2912 (1998)
13. J.-M. Bonard, J.-P. Salvetat, T. Stöckli, W.A. de Heer, L. Forró, A. Chatelain: Appl. Phys. Lett. **73**, 918 (1998)
14. O.M. Küttel, O. Groening, C. Emmenegger, L. Schlapbach: Appl. Phys. Lett. **73**, 2113 (1998)
15. Y. Saito, K. Hamaguchi, S. Uemura, K. Uchida, Y. Tasaka, F. Ikazaki, M. Yumura, A. Kasuya, Y. Nishina: Appl. Phys. A **67**, 95 (1998)
16. S. Fan, M.G. Chapline, N.R. Franklin, T.W. Tombler, A.M. Cassell, H. Dai: Science **283**, 512 (1999)
17. M. Fransen: PhD Thesis, Technical University Delft (1999)
18. T.W. Ebbesen, P.M. Ajayan: Nature **358**, 220 (1992)
19. D. Ugarte, W.A. de Heer, A. Chatelain: Science **274**, 1897 (1996)
20. J.-M. Bonard, T. Stora, J.-P. Salvetat, F. Maier, T. Stöckli, W.A. de Heer, L. Forró, A. Chatelain: Adv. Mater. **9**, 827 (1997)
21. W.K. Maser, J.M. Lambert, P.M. Ajayan, O. Stephan, P. Bernier: Synthetic Metals **77**, 243 (1996)
22. A. Hamwi, H. Alvergnat, S. Bonnamy, F. Béguin: Carbon **35**, 723 (1997); It is worth noting that nanotubes with partly graphitized structure can be produced by catalytic reactions using slightly different growth conditions
23. J.W. Gadzuk, E.W. Plummer: Rev. Mod. Phys. **45**, 487 (1973)
24. S. Frank, P. Poncharal, Z.L. Wang, W.A. de Heer: Science **280**, 1744 (1998)
25. P.J. de Pablo, E. Graugnard, B. Walsh, R.P. Andres, S. Datta, R. Reifenberger: Appl. Phys. Lett. **74**, 323 (1999)
26. W. Zhu, G. Kochanski, S. Jin, L. Seibles: J. Appl. Phys. **78**, 2708 (1995)
27. K. Okano S. Koizumi, S.R.P. Silva, G.A.J. Amaratunga: Nature **381**, 140 (1996)
28. A. Wisitsora-at, W.P. Kang, J.L. Davidson, D.V. Kerns: Appl. Phys. Lett. **71**, 3394 (1997)
29. V.V. Zhirnov, A.B. Voronin, E.I. Givargizov, A.L. Meshcheryakova: Proceedings of the IEEE International Vacuum Microelectronics Conference, IVMC 1995, 340 (1996)
30. B.S. Satyanarayana, A. Hart, W.I. Milne, J. Robertson: Appl. Phys. Lett. **71**, 1430 (1997)
31. C.A. Spindt, I. Brodie, L. Humphrey, E.R. Westerberg: J. Appl. Phys. **47**, 5248 (1976)
32. W.Z. Li, S.S. Xie, L.X. Qian, B.H. Chang, B.S. Zou, W.Y. Zhou, R.A. Zhao, G. Wang: Science **274**, 1701 (1996).
33. S.T. Purcell, V. Thien Binh, N. Garcia: Appl. Phys. Lett. **67**, 436 (1995)
34. J.-M. Bonard, T. Stöckli, W.A. de Heer, A. Chatelain, J.-P. Salvetat, L. Forró: Phys. Rev. Lett. **81**, 1441 (1998)
35. J.-M. Bonard, T. Stöckli, J.-P. Salvetat, L. Forró, A. Chatelain, J.-C. Charlier, X. Blase, A. de Vita, R. Car: unpublished
36. J.P. Barbour, W.W. Dolan, J.K. Trolan, E.E. Martin, W.P. Dyke: Phys. Rev. **92**, 45 (1953)
37. D.L. Carroll, P. Redlich, P.M. Ajayan, J.-C. Charlier, X. Blase, A. De Vita, R. Car: Phys. Rev. Lett. **78**, 2811 (1997)
38. J.W.G. Wildoer, L.C. Venema, A.G. Rinzler, R.E. Smalley, C. Dekker: Nature **391**, 59 (1998); T.W. Odom, J.-L. Huang, P. Kim, C.M. Lieber: Nature **391**, 62 (1998)
39. P. Kim, T.W. Odom, J.-L. Huang, C.M. Lieber: Phys. Rev. Lett. **82**, 1225 (1999)
40. M.S. Dresselhaus, G. Dresselhaus, P.C. Eklund: *Science of Fullerenes and Carbon Nanotubes* (Academic Press, New York 1996)